

Monitoring statistics of the ERS-2 scatterometer for ESA

cycle 92

(Project Ref. 15988/02/I-LG)

Hans Hersbach
European Centre for Medium-Range Weather Forecasts,
Shinfield Park, Reading, RG2 9AX, England
Tel: (+44 118) 9499476, e-mail: dal@ecmwf.int

March 26, 2004

1 Introduction

On 21 August 2003, the world-wide dissemination of ERS-2 data was restarted. Due to a failure of both on-board LBR tape recorders two months earlier, only data is being received for data within the visibility range of a ground station. In practice this limits coverage to the North-Atlantic, part of the Mediterranean, the Gulf of Mexico, and to a small part of the Pacific north-west from the US and Canada (see Figure 2). An initial gap in the North Atlantic was filled by the inclusion of a new ground station at West Freugh (data received at ECMWF since 15 January 2004). Side effect of this inclusion is that certain areas are now reported by more than one station (see report of cycle 91 for details).

The quality of the UWI product was monitored at ECMWF for cycle 92. Results were compared to those obtained from the previous cycle, as well for data received during the nominal period in 2000 (up to cycle 59). No corrections for duplicate observations were applied.

For almost the entire period in cycle 92, the ERS-2 scatterometer data was not used in the 4D-Var data assimilation system at ECMWF. However, a new model cycle was introduced on 9 March 2004, including the assimilation of ERS2 scatterometer data using CMOD5. This means that only for the last 6-hourly period of cycle 92, i.e., for 18 UTC 08 March 2004, ERS-2 scatterometer data was used actively.

During cycle 92, data was received between 21:01 UTC 8 March 2004 and 20:57 UTC 8 March 2004. No data was received for the batches around 06 UTC 11 February 2004 and 06 UTC 18 February 2004 and for 06 UTC 05 February 2004 a

very small amount, all being rejected by the ESA quality control flag.

Mostly, the asymmetry between fore and aft incidence angles was within bounds (3 degrees). Several peaks occurred, the largest (6 degrees) around 02 UTC 1 March 2004. During that event the earth was under the influence of enhanced solar activity.

Compared to cycle 91, the agreement with ECMWF first-guess (FGAT) fields has improved. Relative bias levels became less negative (from -0.61 m/s to -0.51 m/s), and scatter has decreased for the first time since cycle 87 (from 1.71 m/s to 1.67 m/s). Note that seasonal trends for the regional coverage makes a fair comparison difficult. The less optimal results in a relatively small area south-west of the initially data-void area in the Atlantic, as they were observed for cycle 92, were not present anymore for cycle 92.

The quality of de-aliased CMOD4 wind direction was stable, however for the UWI products results were somewhat worse. This indicates that the ESCACA de-aliasing algorithm was working less efficient during cycle 92.

Compared to nominal data in 2000, bias levels for both backscatter and wind speed are more optimal. Standard deviations of wind speed are slightly less optimal to those for 2000. A fair comparison, however, cannot be made due to large differences in data coverage.

The ECMWF assimilation system was changed on 9 March 2004. ERS-2 scatterometer data was re-introduced using CMOD5. Improvements on snow analysis, the usage of GOES AMV, cloud handling in the minimization, the handling of polar vortex instabilities, convection, and on unresolved bathymetry in the ocean-wave model were achieved. For cycle 92 this model upgrade concerned only data for 18 UTC 08 March 2004. Therefore the model change had no effect on results for cycle 92.

The cycle-averaged evolution of performance relative to ECMWF FGAT winds is displayed in Figure 1. Figure 2 shows global maps of the over cycle 92 averaged UWI data coverage and wind climate, Figure 3 the comparison with FGAT.

2 ERS-2 statistics from 3 February to 8 March 2004

2.1 Sigma0 bias levels

The average sigma0 bias levels (compared to simulated sigma0's based on ECMWF model first-guess winds) stratified with respect to antenna beam, ascending or descending track and as function of incidence angle (i.e. across-node number) is displayed in Figure 4.

Compared to cycle 91, bias levels were very similar. Bias levels for ascending tracks have increased by about 0.1 dB. For descending tracks levels became 0.15 dB more negative for the fore beam and up to 0.15 dB higher for the aft beam. The situation is slightly better than that for nominal data in 2000 (see Figure 1 of the reports for cycle 48 to 59). The dependency of the bias as function of incidence angle is small, and most negative in the near range. Compared to cycle 91, internode

differences of the descending tracks have increased somewhat (maximum differences are 0.3 dB). Bias levels are in between 0.2 and -0.5 dB.

The data volume of ascending and descending tracks are nearly equal.

2.2 Incidence angles

For ESACA, across-node binning is, like the old processor, retained on a 25km mesh. From simple geometrical arguments it follows that variations in yaw attitude will lead to asymmetries between the incidence angles of the fore and aft beam. Indeed, this has been observed. Figure 5 gives a time evolution of this asymmetry, showing rapid variations, which are typical for yaw attitude errors. Also in this figure, the occasions for which the combined k_p -yaw quality flag was set are indicated by red stars. The relation with incidence-angle asymmetries is obvious.

From Figure 5 it is seen that during cycle 92 there were several anomalous periods (11, 16, 27 February and 1 March 2004). Only the largest peak (1 March 2004) could be associated with solar activity.

2.3 Distance to cone history

The distance to the cone history is shown in Figure 6. Curves are based on data that passed all QC, including the test on the k_p -yaw flag, however subject to the land and sea-ice check at ECMWF (see cyclic report 88 for details).

Like for cycle 91, time series are (due to lack of statistics) very noisy, especially for the first nodes. This makes it difficult to identify peaks that might indicate a low data quality. Most spikes are a result from low data volumes.

Compared to cycle 91, average levels have increased from 1.17 to 1.21 and are now about 11% higher than for nominal data (see top panel Figure 1).

2.4 UWI minus First-Guess wind history

In Figure 7, the UWI minus ECMWF first-guess wind-speed history is plotted.

The history plot shows many peaks. After 29 February 2004 there is a trend towards more negative bias levels. Similar results apply for the history of de-aliased CMOD4 winds versus FGAT (Figure 9).

Most peaks are a result of low data volume. Other peaks do indicate a real discrepancy between UWI and ECMWF winds, such as for 18 UTC 10 February 2004 and 12 UTC 19 February 2004. For the latter case, the area of largest disagreement is displayed in the top panel of Figure 12. Although not very clear, it seems to indicate a shift in the position of a front. Besides difficulties in the de-aliasing for a patch of winds, the UWI winds do not look erroneous.

Figure 11 displays the locations for which UWI winds were more than 8 m/s weaker (top panel) and more than 8 m/s stronger (lower panel) than FGAT winds. Far lower winds cluster in the area south west of the previously existing data gap. An example is given in the lower panel of Figure 12 (13:16 UTC 27 February 2004).

	cycle 91		cycle 92	
	UWI	CMOD4	UWI	CMOD4
speed STDV	1.71	1.70	1.67	1.65
node 1-2	1.78	1.73	1.74	1.69
node 3-4	1.66	1.65	1.67	1.64
node 5-7	1.64	1.63	1.58	1.57
node 8-10	1.68	1.67	1.61	1.60
node 11-14	1.70	1.70	1.63	1.62
node 15-19	1.69	1.69	1.65	1.65
speed BIAS	-0.61	-0.59	-0.51	-0.49
node 1-2	-1.25	-1.20	-1.13	-1.08
node 3-4	-0.93	-0.86	-0.79	-0.72
node 5-7	-0.64	-0.61	-0.52	-0.48
node 8-10	-0.44	-0.43	-0.37	-0.36
node 11-14	-0.38	-0.37	-0.33	-0.32
node 15-19	-0.39	-0.39	-0.28	-0.27
direction STDV	28.9	19.6	34.3	19.7
direction BIAS	-2.8	-2.9	-2.8	-2.8

Table 1: Biases and standard deviation of ERS-2 versus ECMWF FGAT winds in m/s for speed and degrees for direction

It shows, like the case of the top panel, a shift in the position of a front. The same front was also observed 12 hours earlier (01:05 UTC), indicating a similar relative displacement between the UWI and FGAT winds (not shown).

The distribution of far stronger UWI winds is more concentrated at higher latitudes. Some of them indicate erroneous UWI winds, such as red area near Nova Halifax that are very likely the result from ice-contamination. Others do not show anomalous UWI winds, and just express local differences with FGAT winds, such as the above discussed situation in the top panel of Figure 12.

Average bias levels and standard deviations of UWI winds relative to FGAT winds are displayed in Table 1. From this it is seen that the bias of both the UWI and CMOD4 product have become less negative by 0.1 m/s. Biases are most negative in the near range (see also third panel of Figure 1). The average bias level is less negative than for nominal data in 2000 (UWI: -0.51 m/s now, was -0.79 m/s for cycle 59).

The standard deviation of UWI winds compared to cycle 91 has improved as well (1.67 m/s, was 1.71 m/s). The improvement as function of incidence angle is reasonably homogeneous. Performance is, like for cycle 91 (but not like cycle 90 and before) now worst in the near range.

For cycle 92 the (UWI - FGAT) direction standard deviations were ranging between 20 and 40 degrees (Figure 8). Sharp peaks are the result of low data volumes. For de-aliased CMOD4 winds values between 20 and 30 degrees are most common (Figure 10). Both plots show a transition around 27 February 2004, after which the curves look less volatile and standard deviations seem to decrease.

With respect to cycle 91, the average standard deviation (see Table 1) of the UWI wind direction has increased (34.3 degrees, was 28.9 degrees). The performance of de-aliased CMOD4 winds was stable (19.7 degrees, was 19.6 degrees), indicating that the de-aliasing software of the UWI wind product encountered more troublesome situations than during cycle 91. Bias levels in wind direction were virtually unchanged (- 2.8 degrees unaltered for UWI; -2.8, was 2.9 degrees for CMOD4).

2.5 Scatterplots

Scatterplots of model 10 m first-guess winds versus ERS-2 winds are displayed in Figures 13 to 17. Values of standard deviations and biases are slightly different from those displayed in Table 1. Reason for this is that, for plotting purposes, the in 0.5 m/s resolution ERS-2 winds have been slightly perturbed (increases scatter with 0.02 m/s), and that zero wind-speed ERS-2 winds have been excluded (decreases scatter with about 0.05 m/s).

The scatterplot of UWI wind speed versus FGAT (Figure 13) is very similar to that for (at ECMWF inverted) de-aliased CMOD4 winds (Figure 15). It confirms that the ESACA inversion scheme is working properly. The reduced standard deviation compared to cycle 91 (1.68 m/s, was 1.73 m/s), seems to originate from a better agreement at strong winds between 20 and 25 m/s.

Winds derived on the basis of CMOD5 are displayed in Figure 16. The bias compared to FGAT winds remains small for all wind domains (on average 0.06 m/s, was -0.01 m/s) The relative standard deviation is lower than for CMOD4 winds (1.63 m/s versus 1.66 m/s).

Figure Captions

Figure 1: Evolution of the performance of the ERS-2 scatterometer averaged over 5-weekly cycles from 12 December 2001 (cycle 69) to 8 March 2004 (end cycle 92) for the UWI product (solid, star) and de-aliased winds based on CMOD4 (dashed, diamond). Results are based on data that passed the UWI QC flags. For cycle 85 two values are plotted; the first value for the global set, the second one for the regional set. Dotted lines represent values for cycle 59 (5 December 2000 to 17 January 2001), i.e. the last stable cycle of the nominal period. From top to bottom panel are shown the normalized distance to the cone (CMOD4 only) the standard deviation of the wind speed compared to FGAT winds, the corresponding bias (for UWI winds the extreme inter-node averages are shown as well), and the standard deviation of wind direction compared to FGAT.

Figure 2: Average number of observations per 12H and per 125km grid box (top panel) and wind-climate (lower panel) for UWI winds that passed the UWI flags QC and a check on the collocated ECMWF land and sea-ice mask.

Figure 3: The same as Figure 2, but now for the relative bias (top panel) and standard deviation (lower panel) with ECMWF first-guess winds.

Figure 4: Ratio of $\langle \sigma_0^{0.625} \rangle / \langle \text{CMOD4}(\text{FirstGuess})^{0.625} \rangle$ converted in dB

for the fore beam (solid line), mid beam (dashed line) and aft beam (dotted line), as a function of incidence angle for descending and ascending tracks. The thin lines indicate the error bars on the estimated mean. First-guess winds are based on the in time closest (+3h, +6h, +9h, or +12h) T511 forecast field, and are bilinearly interpolated in space.

Figure 5: Time series of the difference in incidence angle between the fore and aft beam. Red stars indicate the occurrences for which the combined k_p -yaw flag was set.

Figure 6: Mean normalized distance to the cone computed every 6 hours for nodes 1-2, 3-4, 5-7, 8-10, 11-14 and 15-19 (solid curve close to 1 when no instrumental problems are present). The dotted curve shows the number of incoming triplets in logarithmic scale (1 corresponds to 60,000 triplets) and the dashed one indicates the fraction of complete (based on the land-sea mask at ECMWF) sea-located triplets rejected by ESA flags, or by the wind inversion algorithm (0: all data kept, 1: no data kept).

Figure 7: Mean (solid line) and standard deviation (dashed line) of the wind speed difference UWI - first guess for the data retained by the quality control.

Figure 8: Same as Fig. 7, but for the wind direction difference. Statistics are computed only for wind speeds higher than 4 m/s.

Figures 9 and 10: Same as Fig. 7 and 8 respectively, but for the de-aliased CMOD4 data.

Figure 11: Locations of data during cycle 92 for which UWI winds are more than 8 m/s weaker (top panel) respectively stronger (lower panel) than FGAT, and on which QC on UWI flags and the ECMWF land/sea-ice mask was applied.

Figure 12: Comparison between UWI (red) and ECMWF FGAT (blue) winds for a case on 19 February 2004 (top panel) respectively 27 February (lower panel).

Figure 13: Two-dimensional histogram of first guess and UWI wind speeds, for the data kept by the UWI flags, and QC based on the ECMWF ice and land-sea mask. Circles denote the mean values in the y-direction, and squares those in the x-direction.

Figure 14: Same as Fig. 13, but for wind direction. Only wind speeds higher than 4m/s are taken into account.

Figure 15: Same as Fig. 13, but for de-aliased CMOD4 winds.

Figure 16: Same as Fig. 13, but for de-aliased CMOD5 winds.

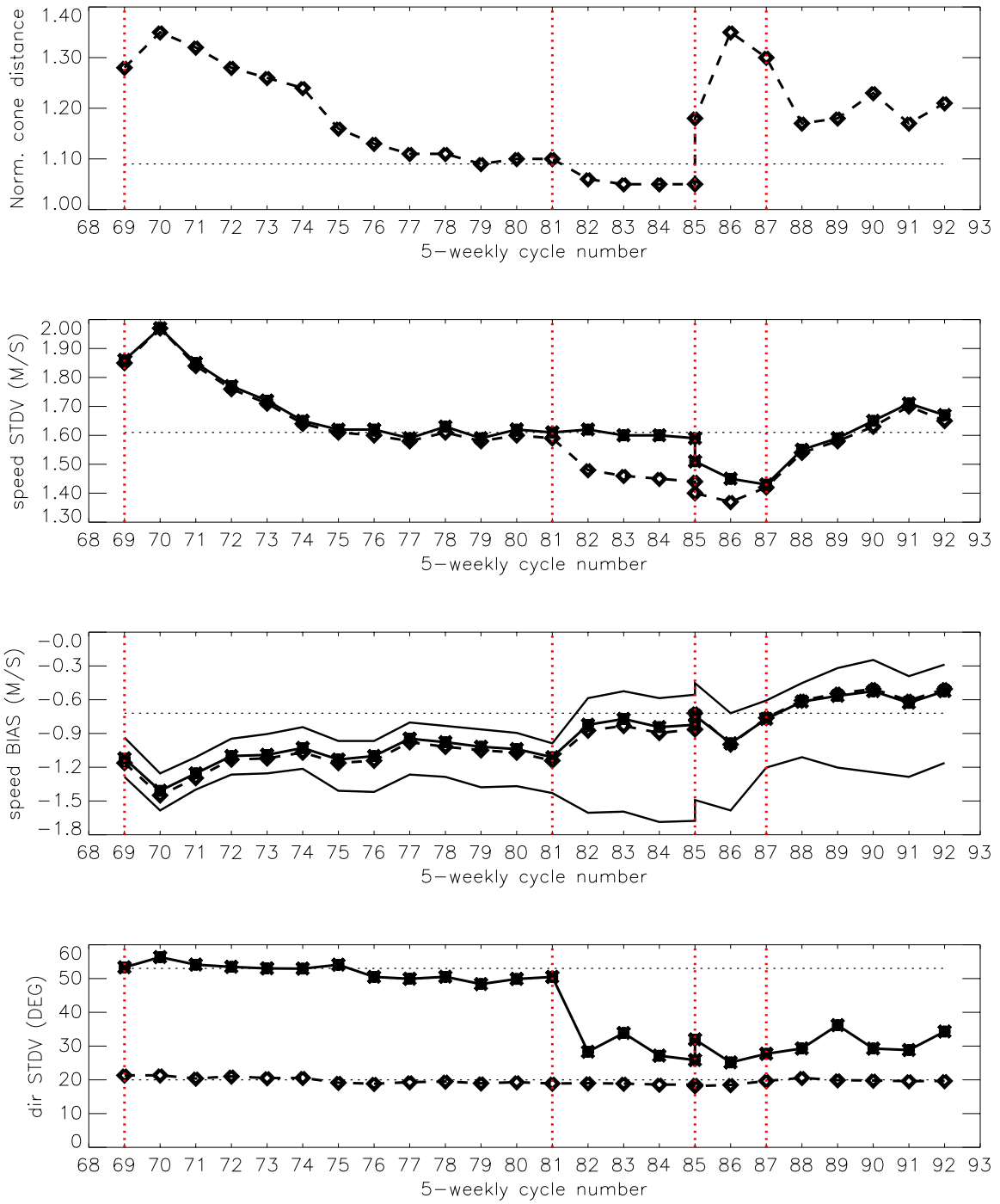
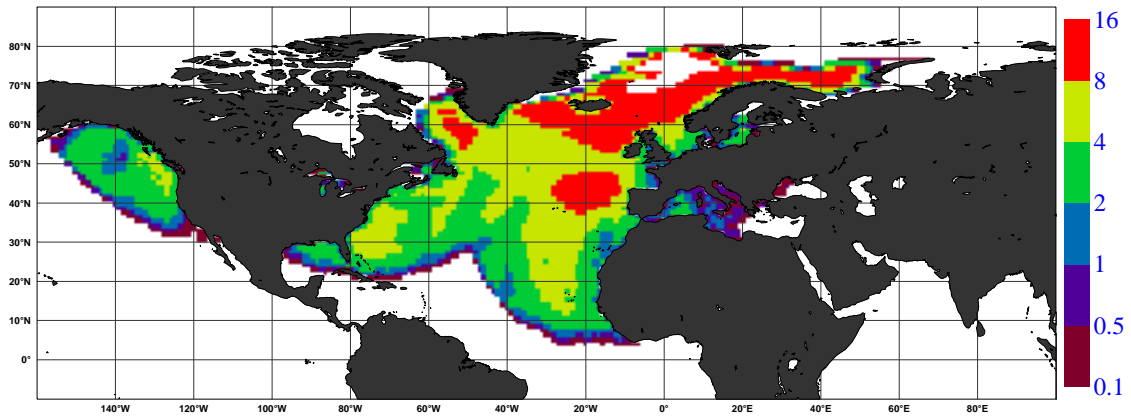


Figure 1

NOBS (ERS-2 UWI), per 12H, per 125km box
average from 2004020300 to 2004030818 GLOB:4.033



AVERAGE (ERS-2 UWI), in m/s.
average from 2004020300 to 2004030818 GLOB:7.62

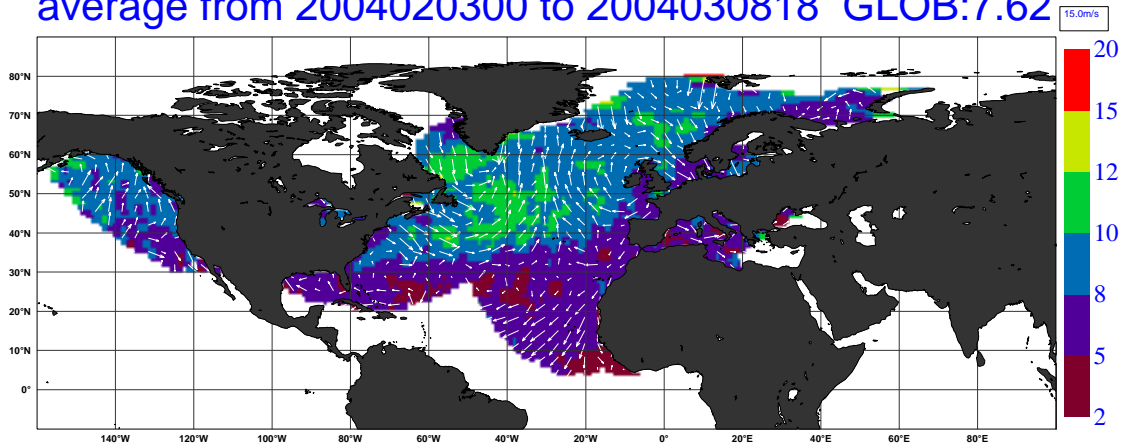
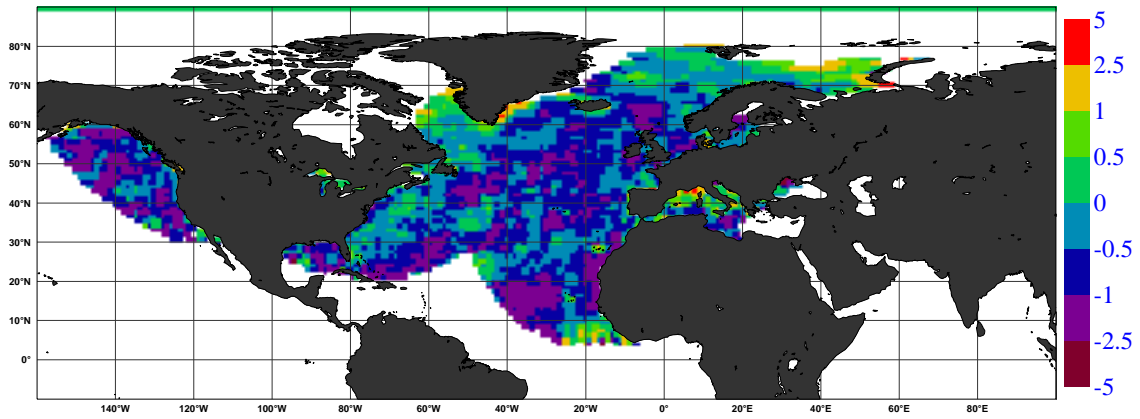


Figure 2

BIAS (ERS-2 UWI vs FIRST-GUESS), in m/s.
average from 2004020300 to 2004030818 GLOB:-0.507



STDV (ERS-2 UWI vs FIRST-GUESS), in m/s.
average from 2004020300 to 2004030818 GLOB:1.423

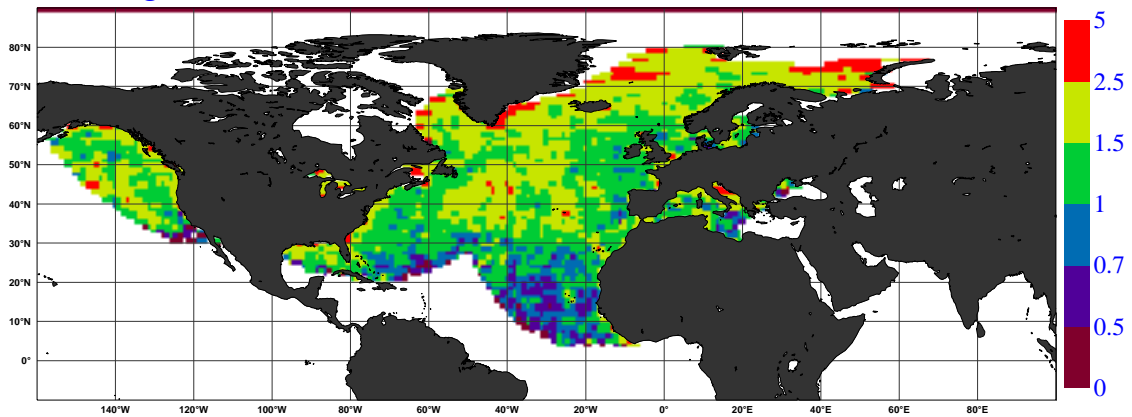


Figure 3

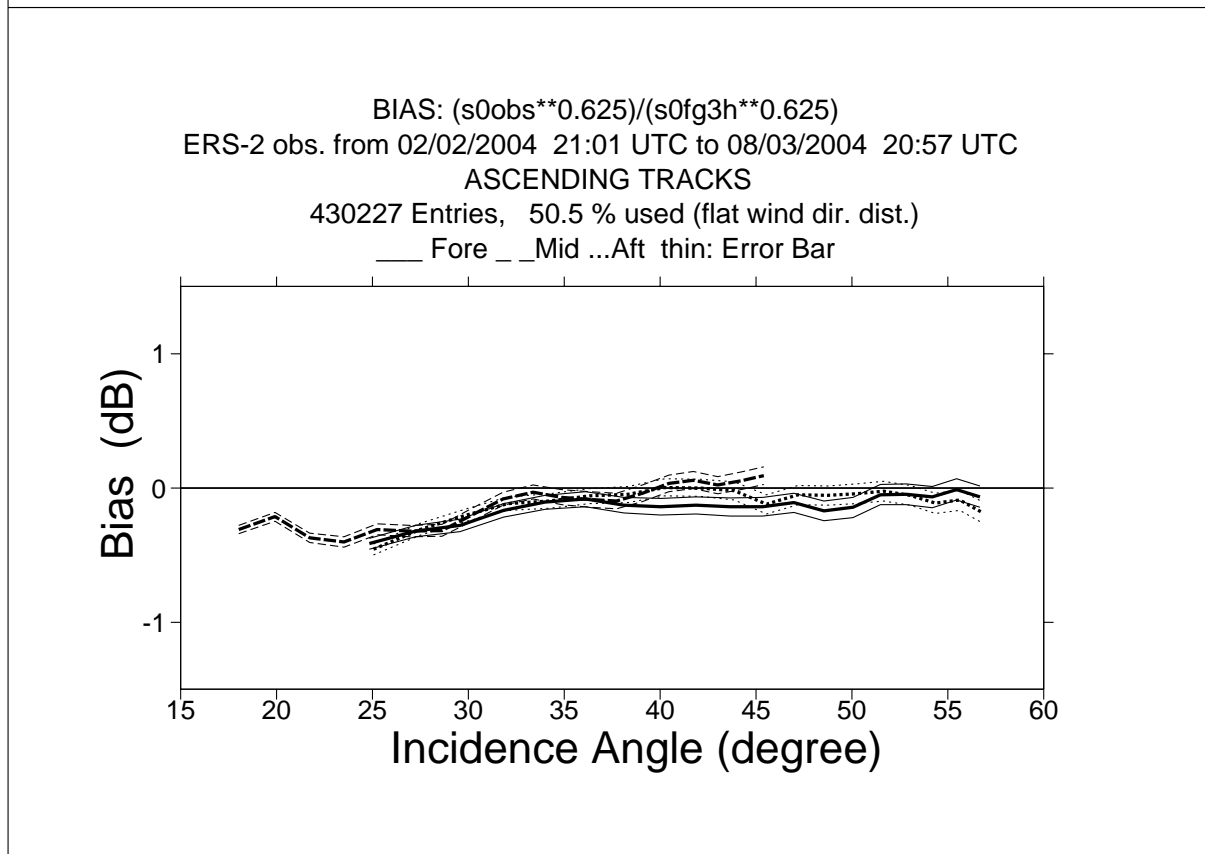
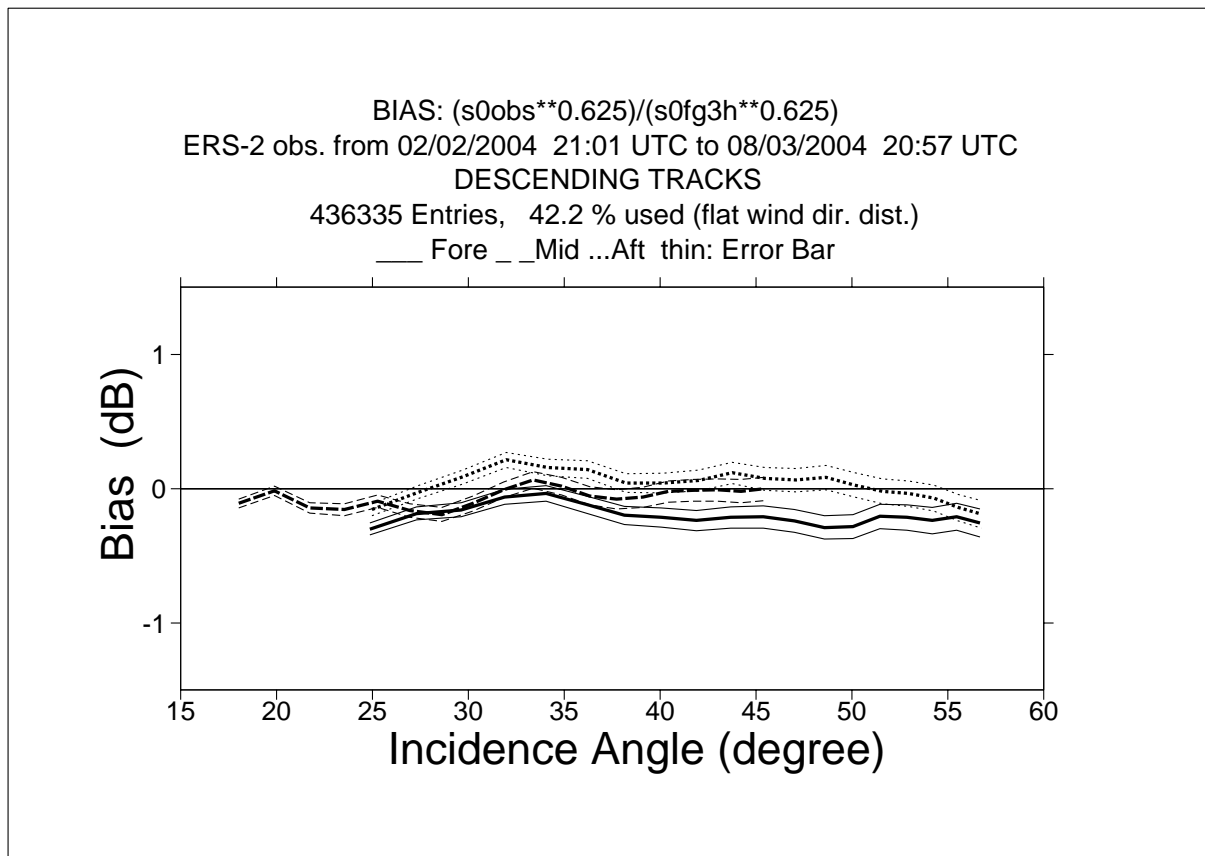


Figure 4

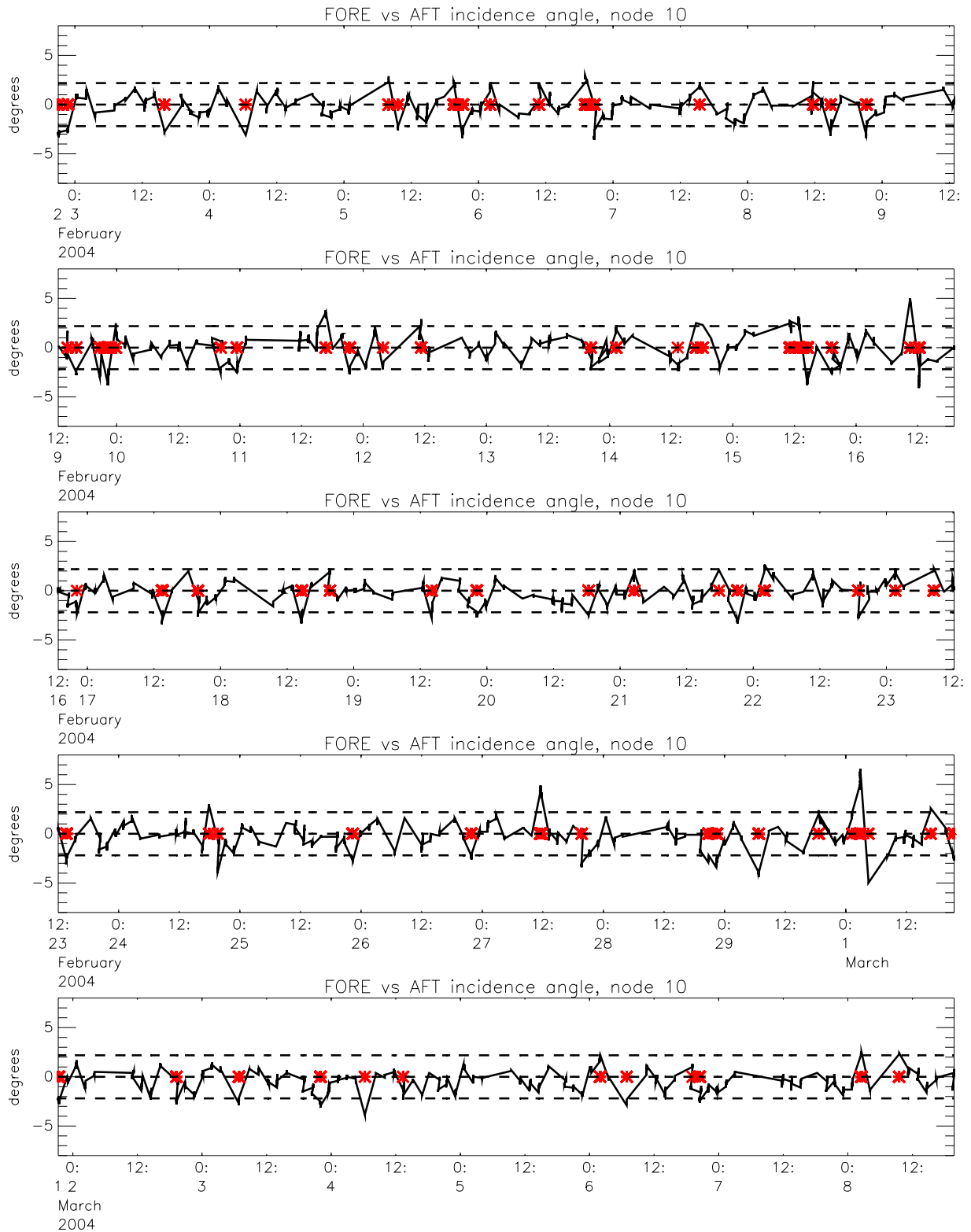


Figure 5

Monitoring of Sigma0 triplets versus CMOD4 for ERS-2

from 2004020300 to 2004030818

(solid) mean normalised distance to the cone over 6 h

(dashed) fraction of complete sea-point observations rejected by ESA flag or CMOD4 inversion

(dotted) total number of data in log. scale (1 for 60000)

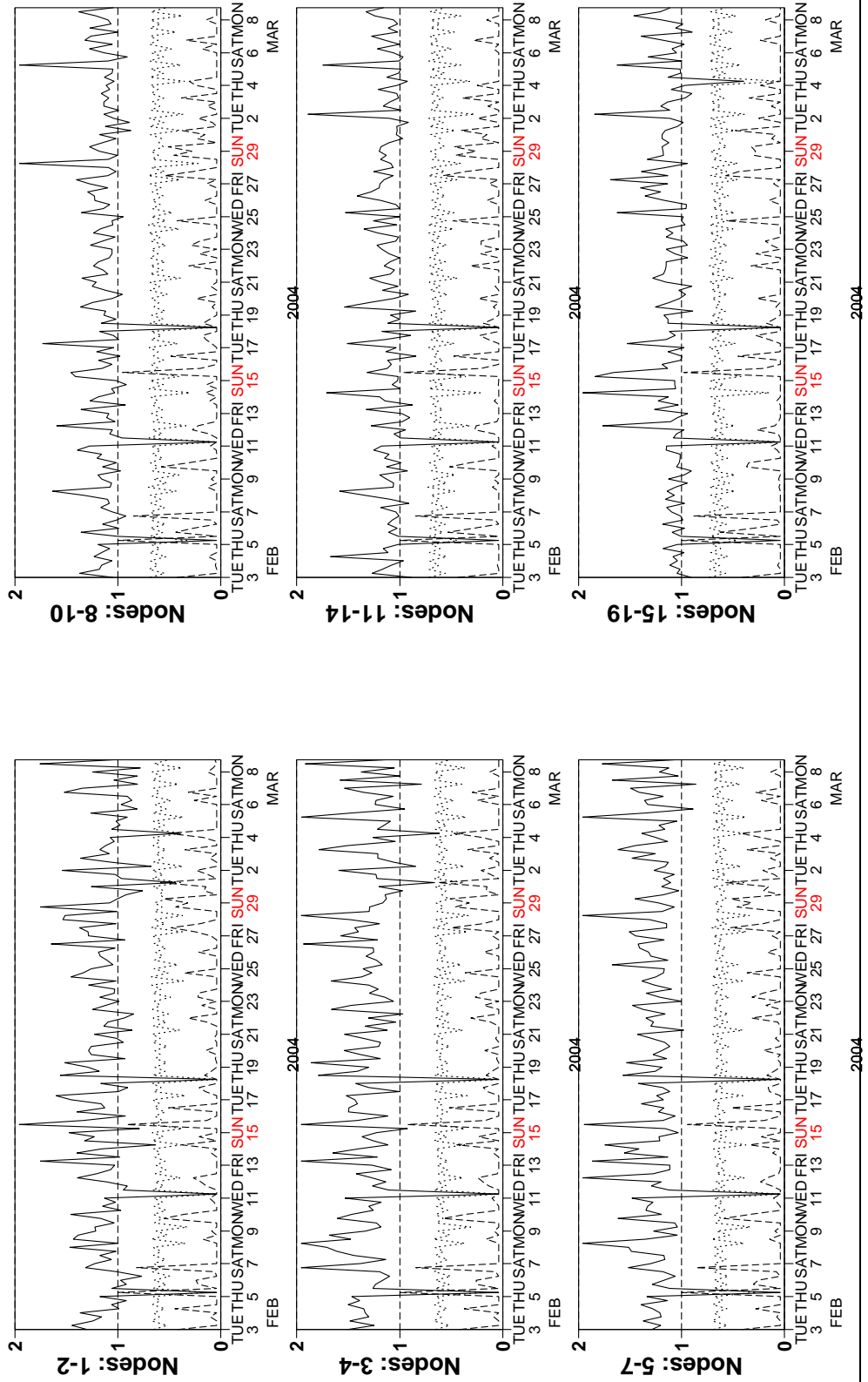


Figure 6

Monitoring of UWI winds versus First Guess for ERS-2

from 2004020300 to 2004030818

(solid) wind speed bias UWI - First Guess over 6h (deg.)

(dashed) wind speed standard deviation UWI - First Guess over 6h (deg.)

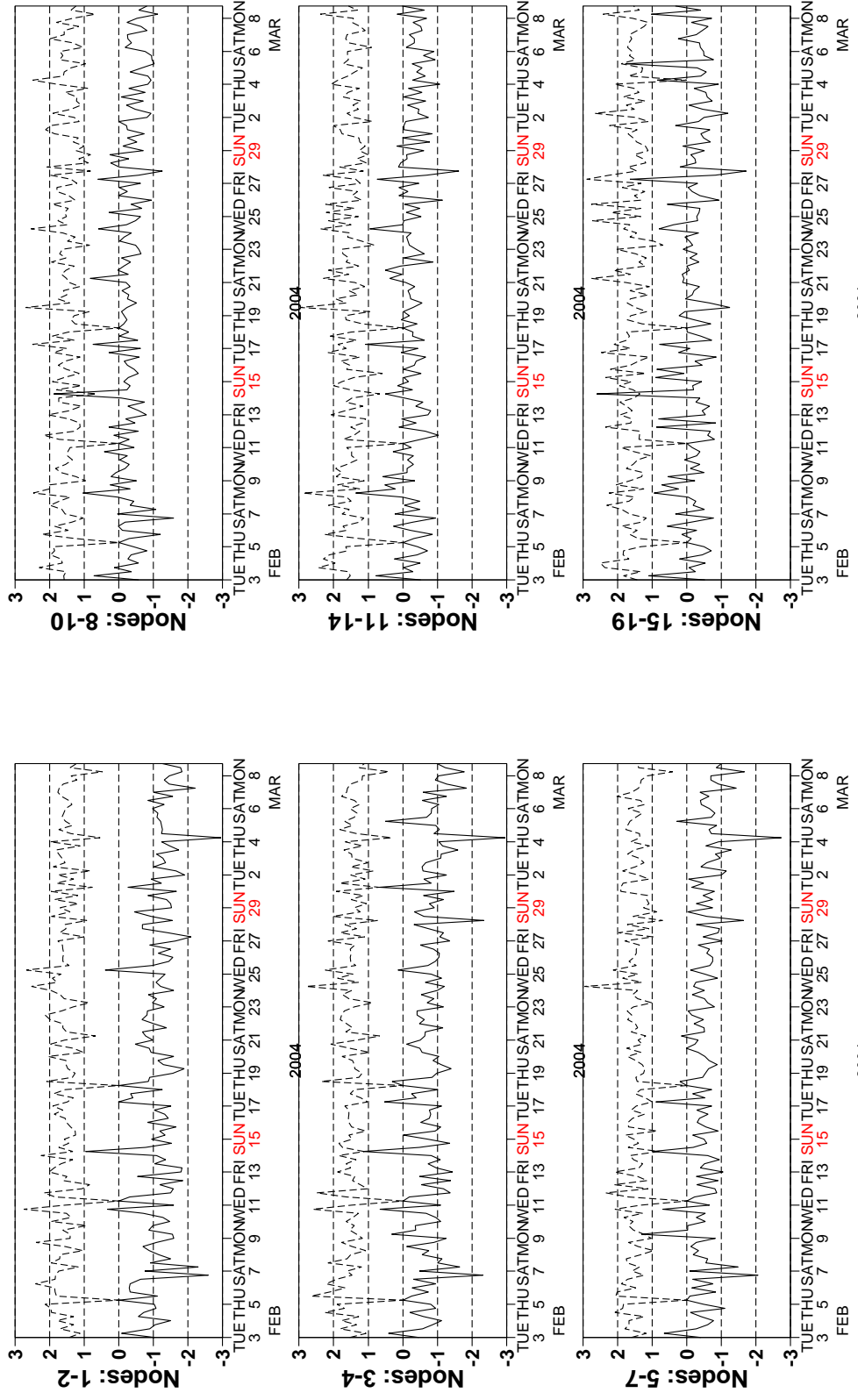


Figure 7

Monitoring of UWI winds versus First Guess for ERS-2

from 2004020300 to 2004030818

(solid) wind direction bias UWI - First Guess over 6h (deg.)

(dashed) wind direction standard deviation UWI - First Guess over 6h (deg.)

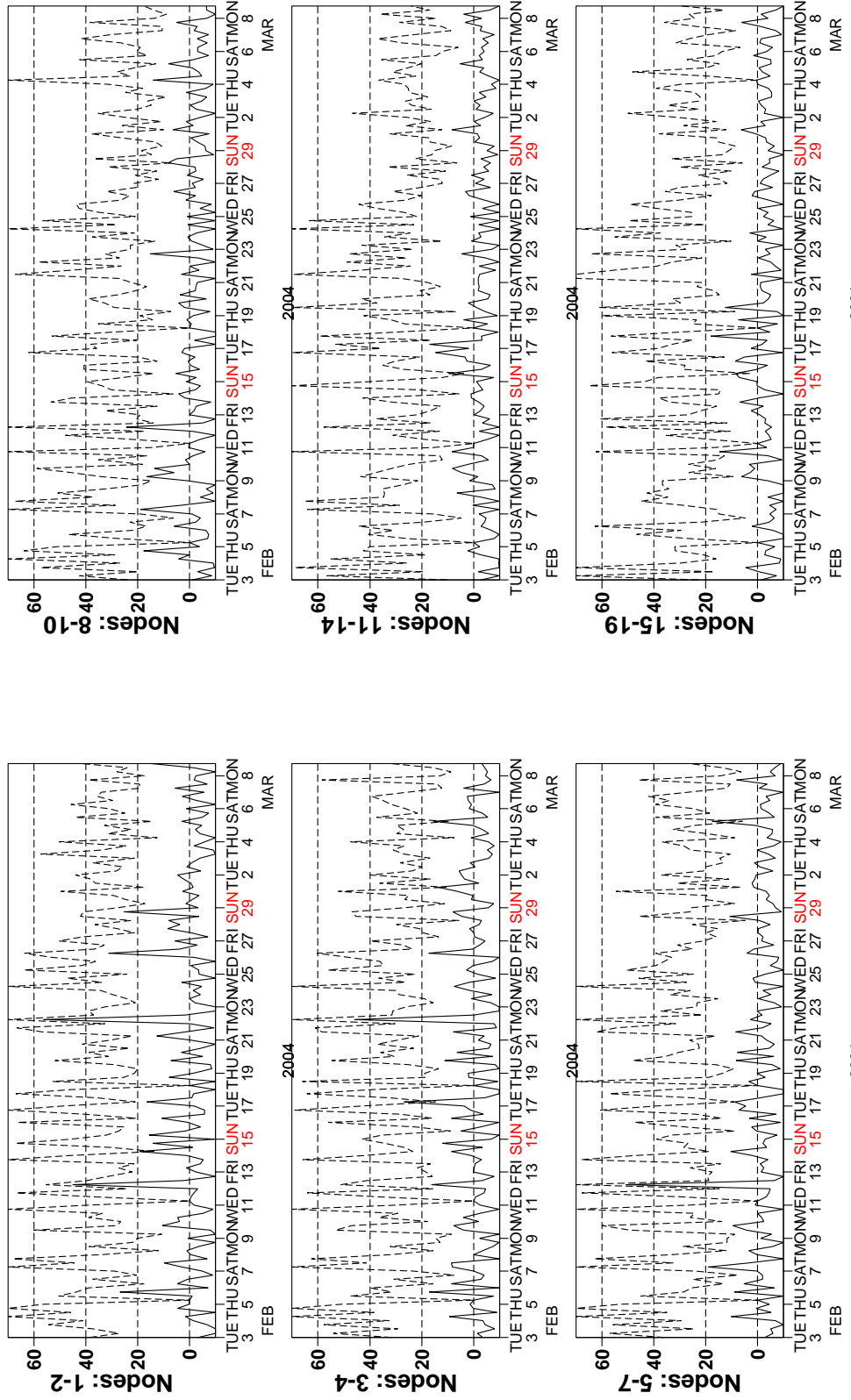


Figure 8

Monitoring of de-aliased CMOD4 winds versus First Guess for ERS-2

from 2004020300 to 2004030818

(solid) wind speed bias CMOD4 - First Guess over 6h (deg.)

(dashed) wind speed standard deviation CMOD4 - First Guess over 6h (deg.)

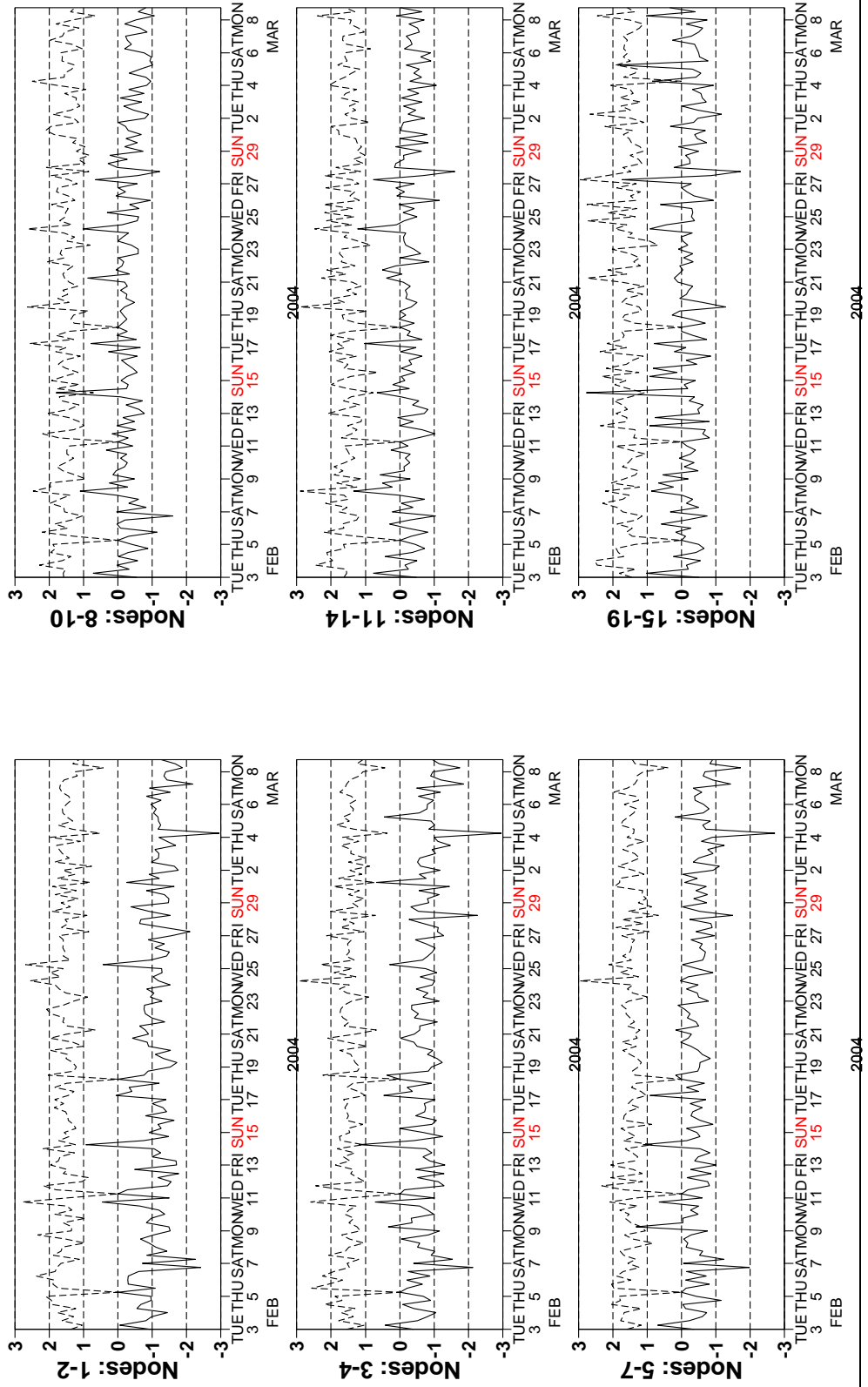


Figure 9

Monitoring of de-aliased CMOD4 winds versus First Guess for ERS-2

from 2004020300 to 2004030818

(solid) wind direction bias CMOD4 - First Guess over 6h (deg.)

(dashed) wind direction standard deviation CMOD4 - First Guess over 6h (deg.)

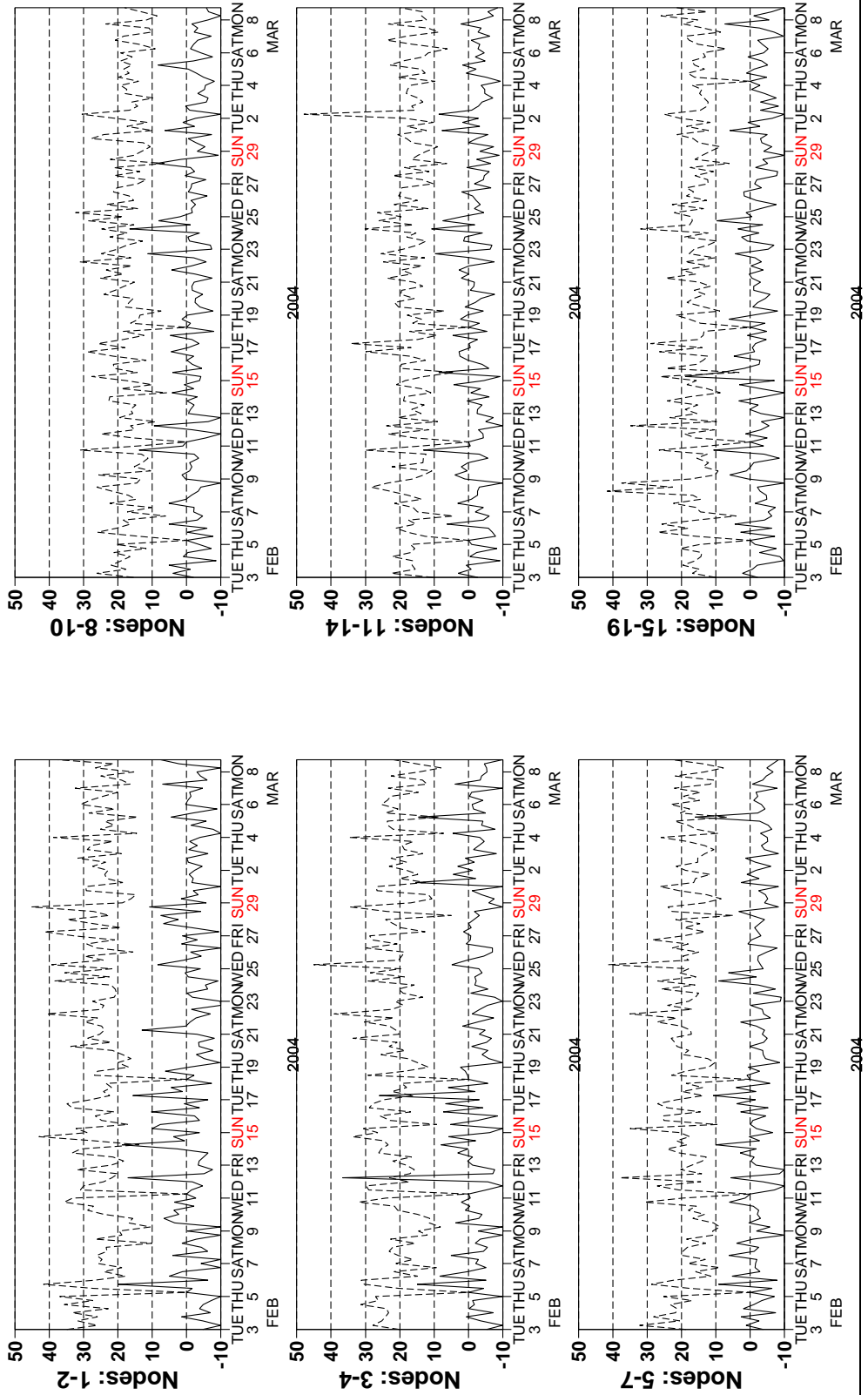
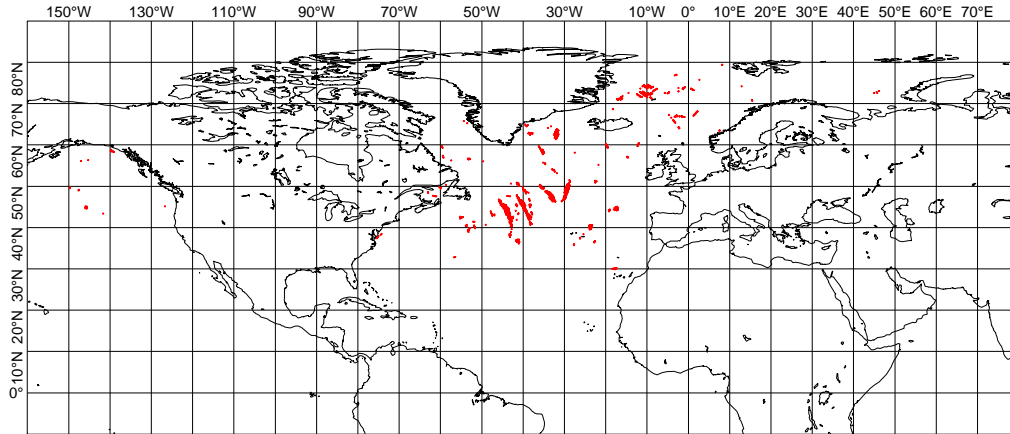


Figure 10

UWI winds more than 8 m/s weaker than FGAT
CYCLE 92, 2004020300 to 2004030818, QC on ESA flags



UWI winds more than 8 m/s stronger than FGAT
CYCLE 92, 2004020300 to 2004030818, QC on ESA flags

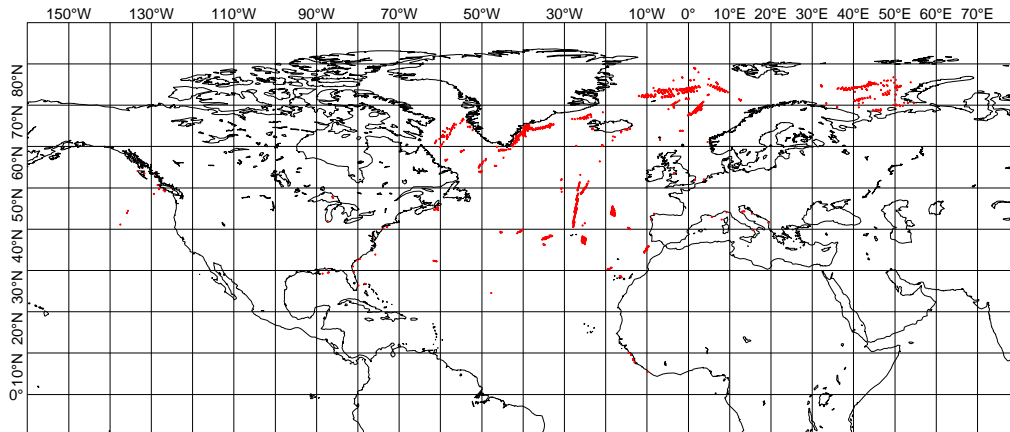
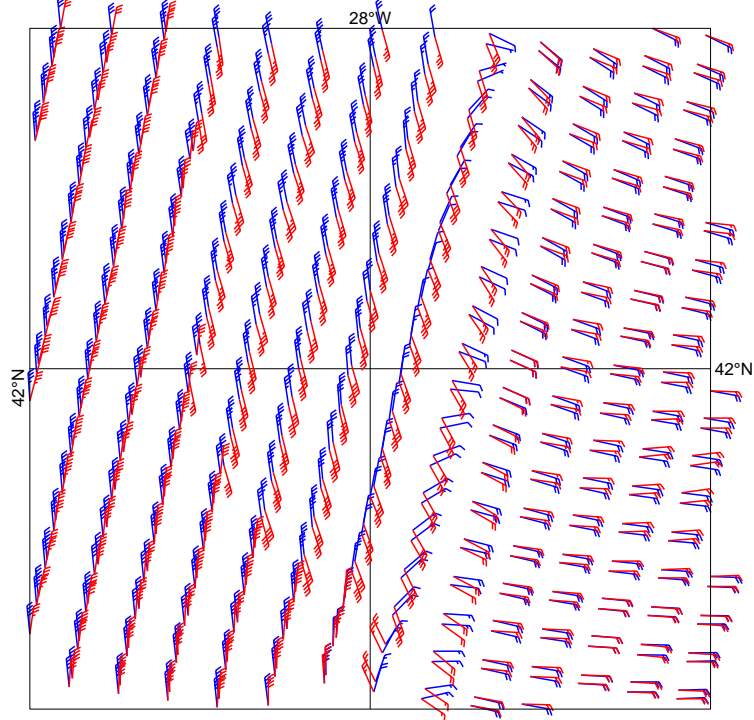


Figure 11

UWI winds (red) versus FGAT winds (blue)
20040219, 12:27 UTC



UWI winds (red) versus FGAT winds (blue)
20040227, 13:16 UTC

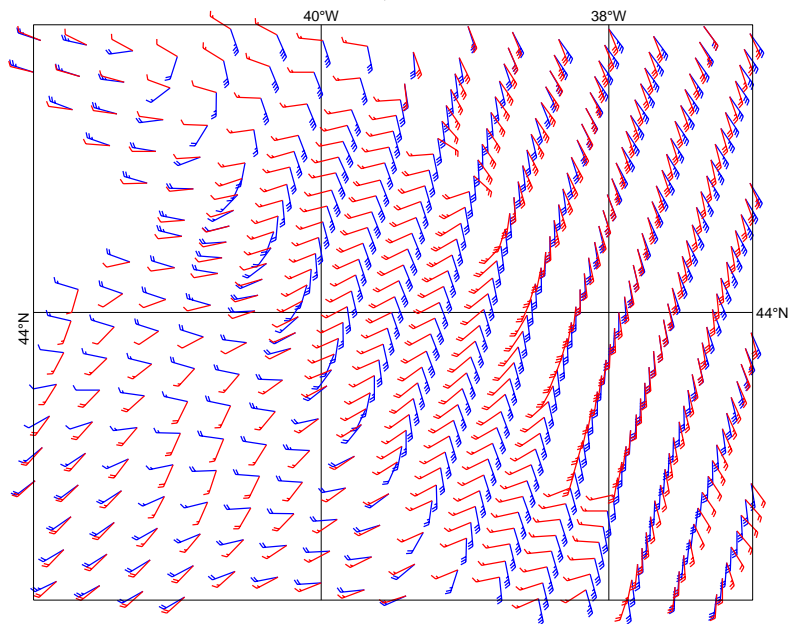


Figure 12

histogram of first guess 10 m winds versus uwi winds
from 2004020300 to 2004030818
= 866562, db contour levels, 5 db step, 1st level at 4.4 db
 $m(y-x) = -0.51$ $sd(y-x) = 1.68$ $sdx = 3.96$ $sd_y = 3.78$ $pcxy = 0.952$

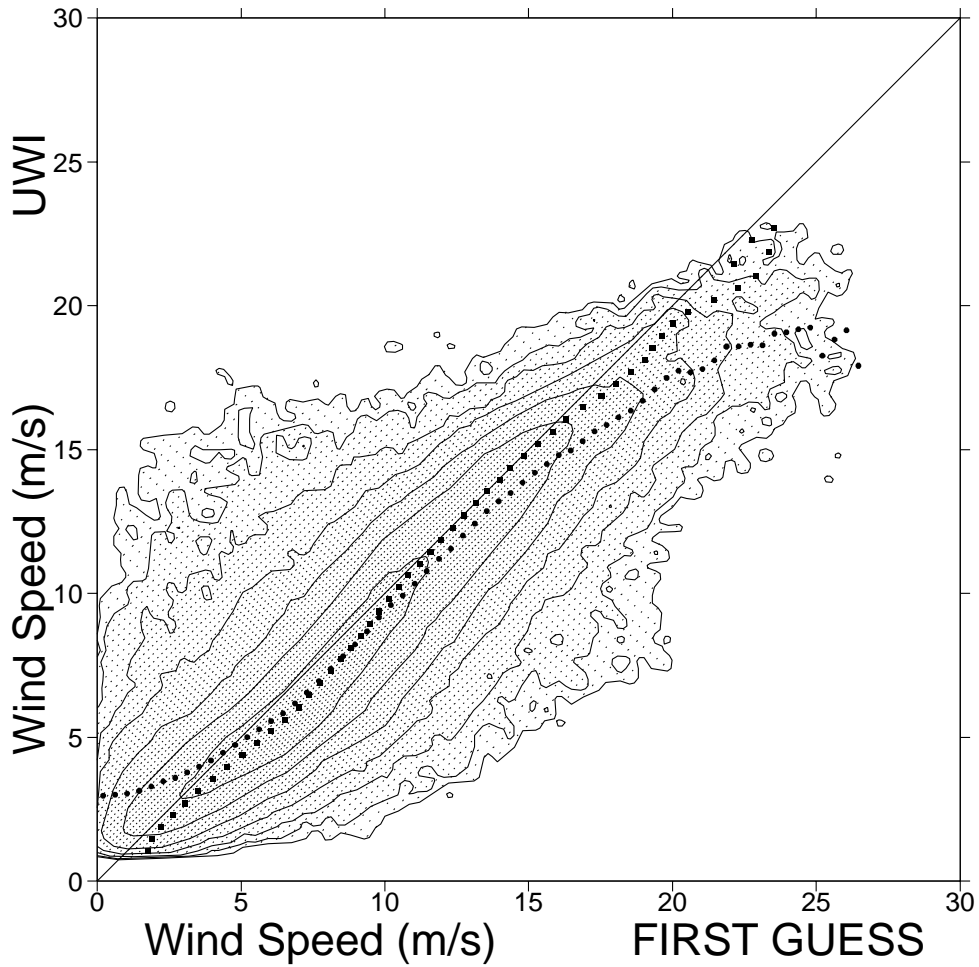


Figure 13

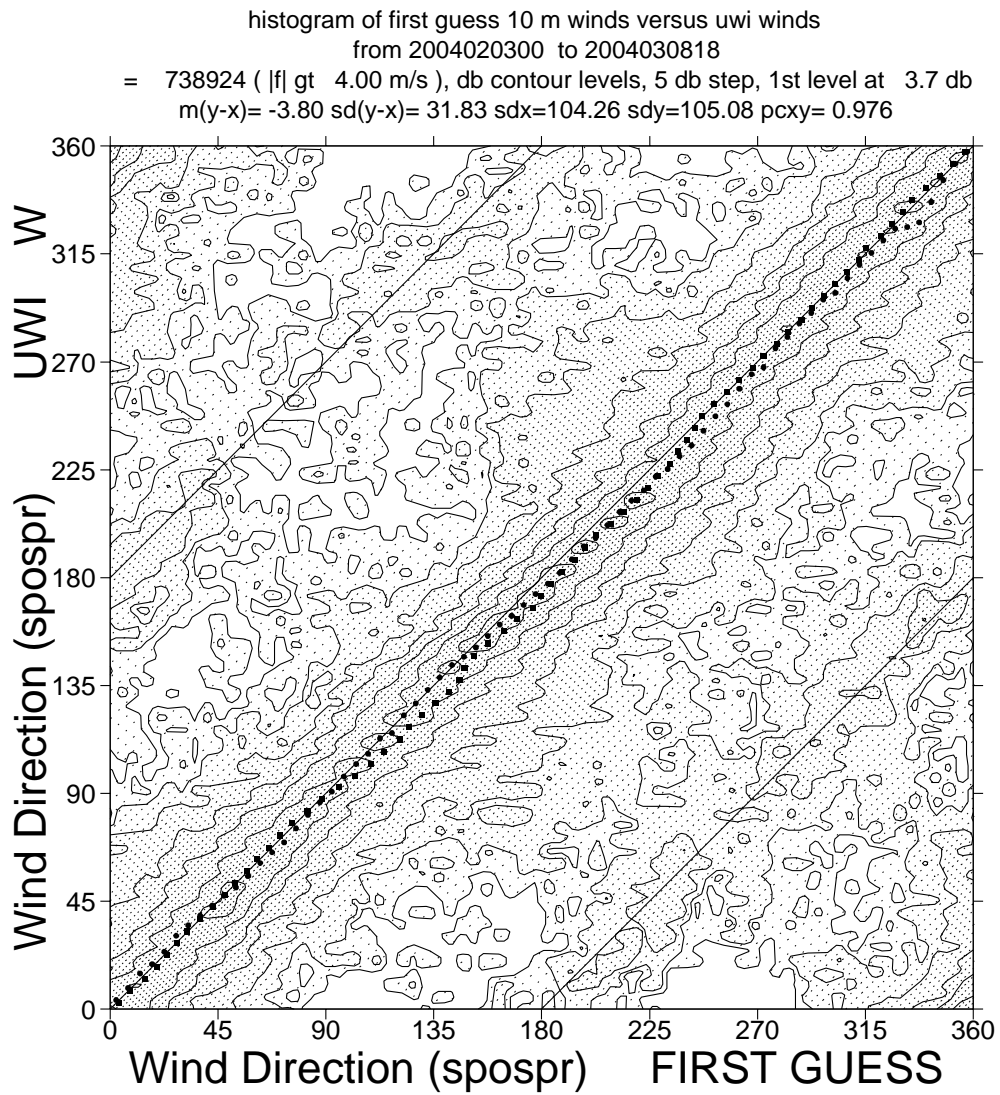


Figure 14

histogram of first guess 10 m winds versus CMOD4 winds
from 2004020300 to 2004030818
= 866216, db contour levels, 5 db step, 1st level at 4.4 db
 $m(y-x) = -0.48$ $sd(y-x) = 1.66$ $sdx = 3.96$ $sd_y = 3.78$ $pcxy = 0.953$

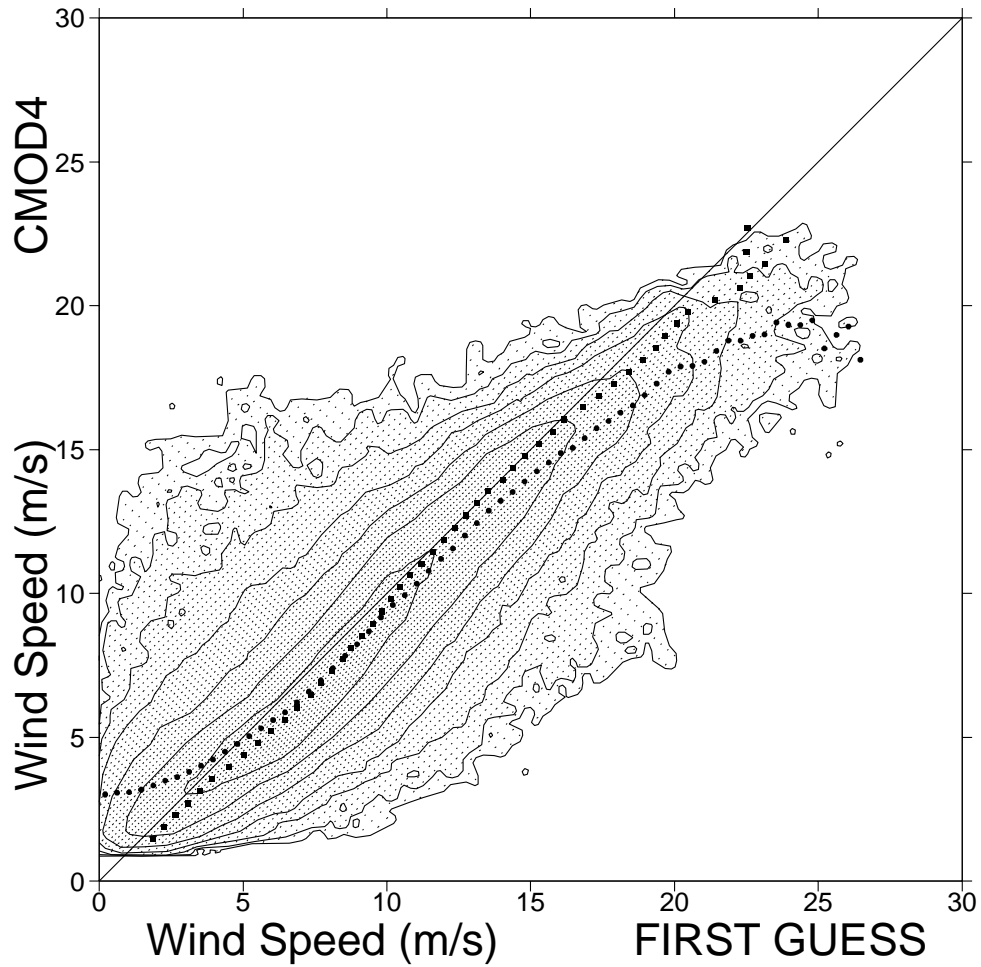


Figure 15

histogram of first guess 10 m winds versus CMOD5 winds
from 2004020300 to 2004030818
= 856937, db contour levels, 5 db step, 1st level at 4.3 db
 $m(y-x) = 0.06$ $sd(y-x) = 1.63$ $sdx = 3.91$ $sdy = 3.84$ $pcxy = 0.955$

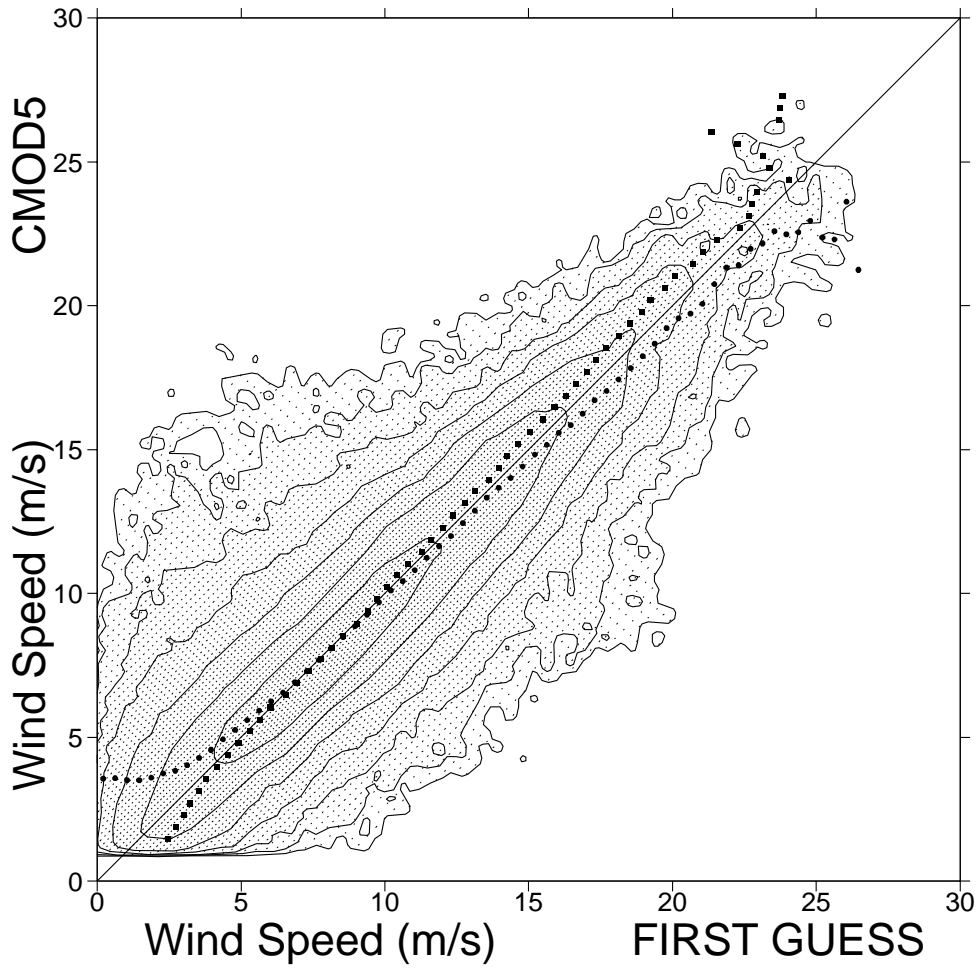


Figure 16